STABILITY PREDICTION ON ARMOR BLOCKS FOR SUBMERGED BREAKWATER BY COMPUTATIONAL FLUID DYNAMICS

Akira Matsumoto[1], Akira Mano[2], Jun Mitsui[1] and Minoru Hanzawa[3]

An evaluation model of the critical condition on armor block stability for submerged breakwaters was proposed by Matsumoto et *al*. (2011). However, the effect of the force normal to the block was not included in the model. Moreover, the drag and inertia coefficients were set to 1.0 as tentative values. In this study, the proposed model is improved by the inclusion of the wave force in the normal direction and the use of the fluid force coefficients determined by a 3-D numerical computation.

Keywords: wave force, stabilizing force, Morison formula, numerical wave flume

INTRODUCTION

Breakwaters, such as detached or submerged breakwaters, are the most fundamental structures to protect coastal areas from wave action. In recent years, submerged breakwaters are increasingly constructed not only to dissipate wave energy but also to preserve the natural landscape. The submerged breakwaters are exposed to high breaking waves and their stability requires fundamentally large stones or concrete blocks. In Europe, it is possible to obtain natural stones with masses reaching 10 ton (CIRIA, 1991). Therefore the armoring materials appearing in the literature are of natural stones (e.g., Van der Meer and Pilarczyk, 1990; Vidal et *al*., 1995, 2000). On the contrary, in Japan, since natural stones heavier than 2 to 3 ton are not easily available, flat type concrete blocks are inevitably used as the armoring materials.

To ensure the stability of a whole structure of a submerged breakwater, it is of prime importance to determine the required mass of the armor blocks accurately. To find the stability number of the blocks used in the Hudson formula (Hudson, 1959), experimental studies were conducted by many researchers, for example, Asakawa et *al*., 1992; Nakayama, 1993; Okamoto and Kawano, 1993. Although the validity of the Hudson formula has been well recognized through numerous construction experiences, the accuracy and range of applicability of the formula have been left unsolved. As the stability number Ns is decided by the results of experiment, a limitation of application of the formula is inevitable depending on the experimental conditions. If the design condition is out of the range of application, model experiments have to be conducted. However, it is very time consuming to determine the optimum mass of armor blocks.

In this context, Matsumoto et *al*. (2011a) proposed a new evaluation model of the critical condition on armor block stability. The method is based on a wave induced flow field around a breakwater, which is calculated by a numerical wave flume CADMAS-SURF (Isobe et *al*., 1999), and successive wave force calculation based on the Morison formula. Trial computation and comparison with experimental results demonstrate the validity and usefulness of the proposed method. However, the effect of the force normal to the block is not included in the model. Moreover, the drag and inertia coefficients are set to 1.0 as tentative values. In this study, the proposed model is improved by the inclusion of the wave force in the normal direction and the use of exact fluid force coefficients.

HYDRAULIC MODEL EXPERIMENT

Wave Force Measurement

A light concrete block stabilized by distributed holes, hereafter referred to as the five-hole block (Matsumoto et *al*., 2011b), was used as an example of a concrete armor unit. The following is a summary of the results of the hydraulic model experiments.

Figure 1 shows the experimental setup for wave force measurement. The horizontal and vertical wave force acting on the block placed at the seaward edge of the crown and the top of the slope were measured. Two types of the blocks were used for the test to investigate the effect of the holes on the forces acting on the block. One was a five-hole block and the other a block with no holes (no-hole

[1] Technical Research Institute, Fudo Tetra Corporation, 2-7 Higashi-Nakanuki, Tsuchiura, 300-0006, Japan
[2] International Research Institute of Disaster Science, Tohoku University, 6-6-06 Aoba, Sendai, 980-8579, Japan
[3] Block and Environment Dept., Fudo Tetra Corporation, 7-2 Koamicho, Nihombashi, Chuo-ku, 103-0016, Japan

block). Regular wave with a period of 2.0s was used. The submerged depth R was determined to be 2.0cm by referring to actual site conditions (Noguchi et *al*. 2002).

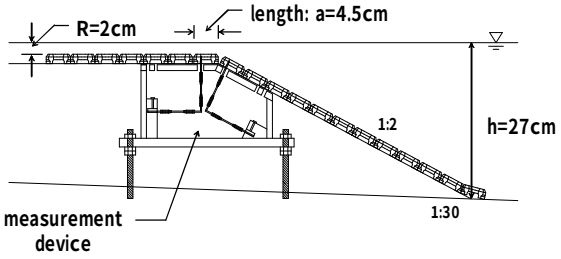

Figure 1. Experimental setup for wave force measurement.

Figure 2(a) shows the hodograph of the wave force acting on the block at the seaward edge of the crown. The horizontal and vertical axes represent the normalized wave forces where F_x and F_z are the wave forces in the tangential and normal direction respectively, ρ_w is the density of water, g is the gravitational acceleration, D_n is the nominal diameter of the five-hole block ($D_n = V^{1/3}$), V is the volume of the five-hole block. The vertical wave force acting on the five-hole block is smaller than that acting on the no-hole block. The vertical force acting on the five-hole block was reduced effectively. The horizontal force acting on the five-hole block was a little larger than that acting on the no-hole block. Figure 2(b) shows the hodograph of wave force acting on the block at the top of the slope. At this position, in contrast to the seaward edge of the crown, the direction of the normal force was downward whenever waves attacked. This contributed to increased block stability.

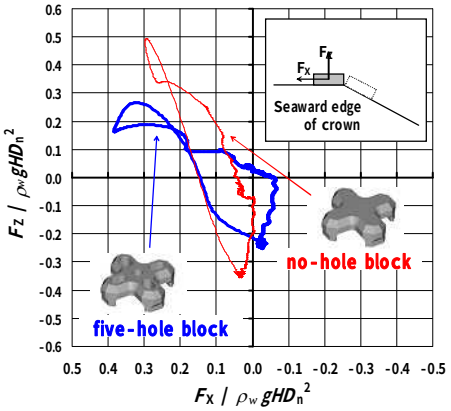

(a) Seaward edge of the crown

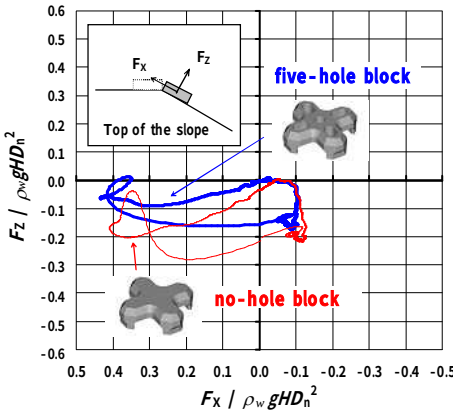

(b) Top of the slope

Figure 2. Hodograph of wave force.

Stability Tests

A series of stability tests were conducted in a 55m-long, 1.2m-wide and 1.5m-deep wave flume. The submerged breakwater model was situated on a 1:30 bottom. The test conditions are summarized in Table 1 and the test sections are shown in Figure 3.

The rubble mound consisted of 0.06-1.50g stones to model the prototype submerged breakwater. The test started with small waves with no block damage and the wave height was gradually increased. The number of waves for each wave height rank was set to approximately 1000. After wave attack with each wave height rank, the test section was not rebuilt. In these tests, damage was defined as when a block had moved more than half of its length from its initial position, rotated more than 45 degrees, and lifted up more than its height.

Table 1. Experimental conditions of stability tests.

Model scale	1/52
Bottom slope	1/30
Water depth *h*	25cm
Submerged depth *R*	2, 4, 6, 8, 10 cm
Crown width *B*	100cm
Offshore slope of breakwater	1 : 2
Frequency spectrum	Modified Bretschneider and Mitsuyasu type
Significant wave period $T_{1/3}$	1.5, 2.0 s
Mass of armor block *M*	29.3 g
Length of armor block *a*	4.5cm
Thickness of armor block *D*	1.62cm
Density of armor block ρ_r	2.3g/cm^3

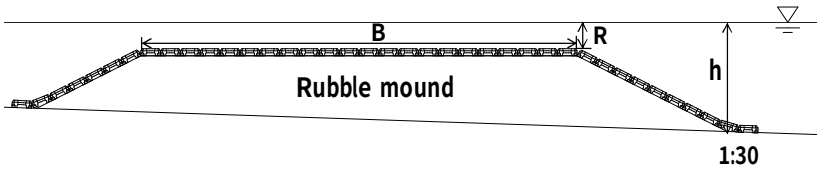

Figure 3. Model test section for stability tests.

Figure 4 shows the possible existence range of the critical stability number obtained by the experiment. The stability number is defined as follows:

$$Ns = \frac{H_{1/3}}{\left(\rho_r / \rho_w - 1\right) D_n} \tag{1}$$

where $H_{1/3}$ is the significant wave height, ρ_r is the density of the block. In Figure 4, two points, *i.e.*, the maximum stability number without damage and the minimum stability number with damage are connected by the solid line. Therefore the critical stability numbers exist somewhere on these lines. Although the data show scatter, increased stability with increase in normalized submerged depth is observed. The average value of the experimental data is also shown. The hatched area expresses the stability numbers of existing conventional blocks. The stability of the five-hole block had improved significantly in comparison with the conventional blocks.

Generally, initial damage to conventional blocks occurs at the seaward edge of the crown. The damage is caused by rotation. However the initial damage to the five-hole block did not occur at the seaward edge of the crown. It was observed rather that the block located at the top of the slope or on the slope tended to move. This agrees with the results of the wave force measurements. The new block placed at the seaward edge of the crown decreased the uplift force effectively. Rubble stones at the seaward edge of the crown gradually moved so as to form round shapes. The discontinuous edge disappearing leads to the increase in block stability. When the breaking waves acted on the rubble mound directly, the small size stones were sucked out through the holes in the five-hole block. However the total number of stones sucked out was few. The sucking effect therefore did not cause a large deformation of the rubble mound.

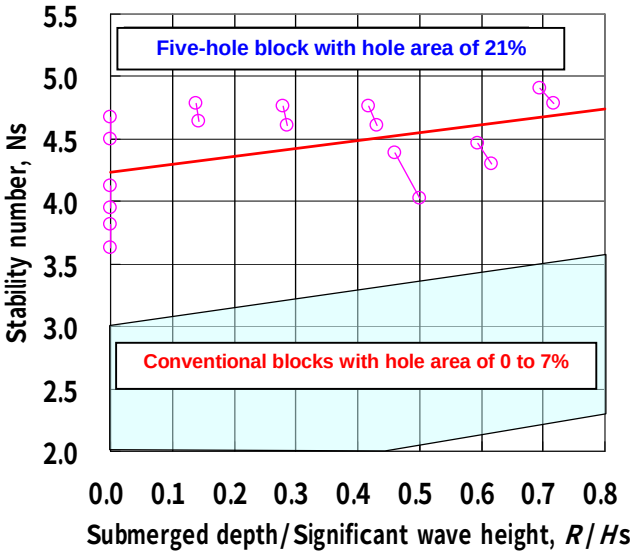

Figure 4. Results of stability tests.

METHODOLOGY OF STABILITY PREDICTION

Fundamental Concept

Based on the characteristics of the damage to armor blocks observed in the hydraulic model experiment, an evaluation method was derived. As for the armor blocks used for the submerged breakwater, a simplified theory on the drag and inertia force indicated the increased significance of the inertia force. Accordingly, the wave force acting on the armor block was calculated by Morison formula taking into account both the flow velocity and the acceleration of the flow. The stability of the armor block was judged by a comparison between the wave force and the stabilizing force originating from the mass of the armor blocks. This methodology is different from the conventional estimation method based on the Isbash number, (for example, Okuma et *al*., 2003; Kondo et *al*., 2009) in which only the drag force is taken into account. To formulate an accurate estimation method, the following points were considered.

(a) Because the flow acting on a block installed at a particular position is affected by adjacent blocks in upstream positions, a coefficient to express such a shading effect was introduced.
(b) To model the structural weakness of the armor block at the top of the slope, the stabilizing force there was decreased.
(c) Damage to the armor blocks did not originate with a maximum wave alone but correlated to the repetition of wave action. For example, Yamamoto and Asakawa (1982) proposed the use of one-tenth the highest wave height $H_{1/10}$. On the other hand, Van der Meer et *al*. (1991) used the two percent non-exceeding wave height $H_{2\%}$. According to the recommendation in these, the one-tenth of the highest wave force was used for the formulation in this study.

Fluid Force Coefficients

Drag, inertia and lift force coefficients C_D, C_M and C_L were obtained by using the three dimensional numerical computation. An open source CFD software “Open FOAM” (Open CFD Ltd., 2011), which can treat the complicated 3-D block geometry under the unstructured computational grid system, was successfully used to reproduce the 3-D flow field around the armor block. Figure 5 shows the computational grid and the placement of the armor blocks. Regular wave with a wave period of 2s and wave height of 4cm were used. The submerged depth was fixed to 2cm.

Then the following two time series of the fluid force acting to the armor block were obtained. One was a summation of the pressure acting on the surface of the block. The other was obtained by applying the computed flow velocity to the Morison equation expressed by Eqns.2 and 3. The computed flow velocity was obtained at the position 0.5cm above the armor block.

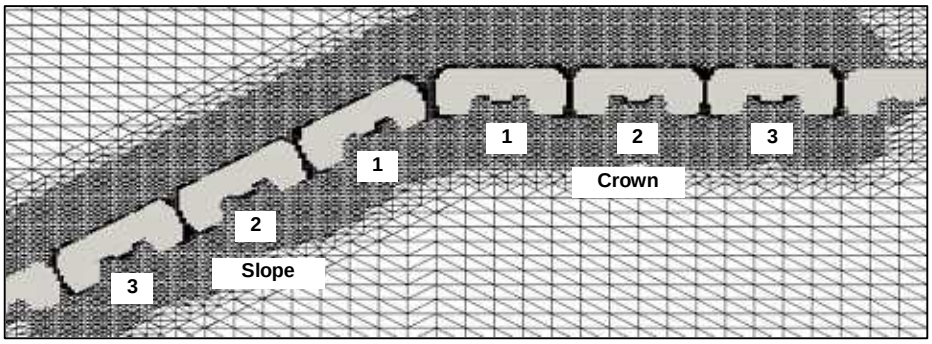

Figure 5. Grid system and the placement of the armor blocks.

$$F_t = \frac{1}{2} C_D \rho_w S_t u_t |u_t| + C_M \rho_w V \frac{du_t}{dt} \tag{2}$$

$$F_n = \frac{1}{2} C_L \rho_w S_n u_t |u_t| \tag{3}$$

where u_t is the flow velocity in the tangential direction of the block, S_t and S_n are the areas of projected plane of the armor block in the tangential and normal direction. The rubble mound was treated as a porous structure. Calculation conditions are summarized in the Table 2.

The values of the fluid force coefficients were determined in such a way that the residual error could be minimized. The drag coefficient C_D and the inertia coefficient C_M were decided based on the analysis of the tangential wave force whereas the lift coefficient C_L was decided by the results of normal force. Figure 6 shows a comparison between these two time series of wave forces. The fluid force coefficient varies from place to place. However, the maximum values appeared at the top of the slope and the offshore end of the crown. These values were therefore adopted as the representative values for the blocks on the slope and the crown. The resultant fluid force coefficients were set as C_D = 1.2, C_M = 0.6, C_L = –0.3 for the slope and C_D = 0.8, C_M = 0.9 and C_L = – 0.1 for the crown.

As for the expression of the normal wave force F_n, the effect of the direction of the flow is included as shown in Eq.3. The reason for this is the influence of the geometry of the submerged breakwater mound itself. Fluid force coefficients are not obtained by putting a single block in a steady flow but are obtained by placing armor blocks in the submerged breakwater. Therefore the direction of the normal force is dependent on the direction of the tangential force as shown in Figures 7 and 8.

Table 2. Calculation conditions of 3-D numerical computation.

Discretization method	Finite volume method
Computational grid	Unstructured collocated grid
Solution algorithm for Navier-Stokes equation	PISO algorithm
Discritization method for advection term	TVD scheme (second-order accuracy)
Turbulence model	RNG-kε model
Time step	Automatic
Boundary conditions	
Bottom boundary, Surface of the block	No-slip
Lateral boundary	Slip
Upper boundary	Open boundary
Resistance force model	Dupuit-Forcheimer law
Material constant of rubble stone α_0, β_0	1500, 3.6
Porosity of rubble mound	0.4
Nominal diameter of rubble stones	0.01m

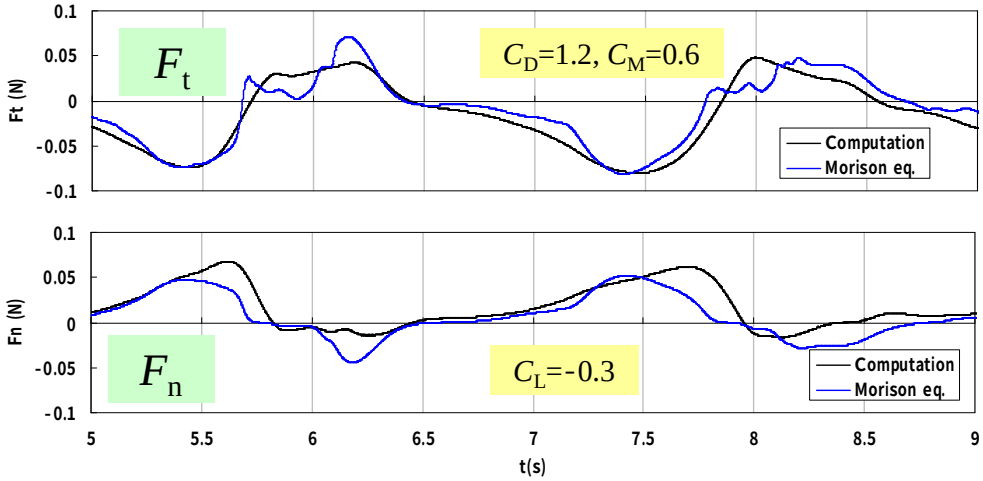

Figure 6. Time series of wave forces by numerical computation and Morison equation. (Armor block place at the top of the slope)

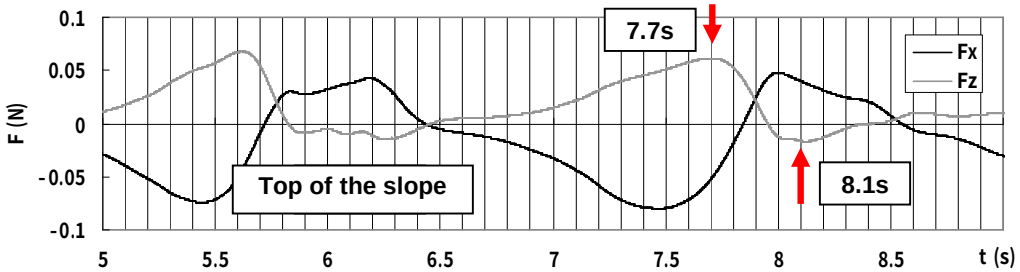

Figure 7. Time series of tangential and normal wave forces by numerical computation. (Armor block place at the top of the slope)

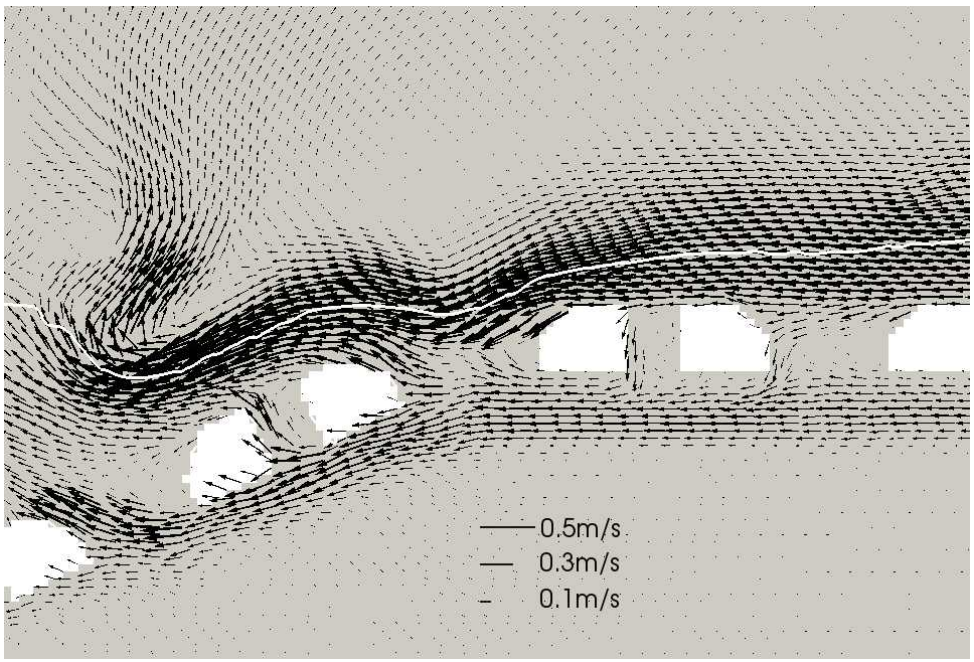

(a) t=7.7s

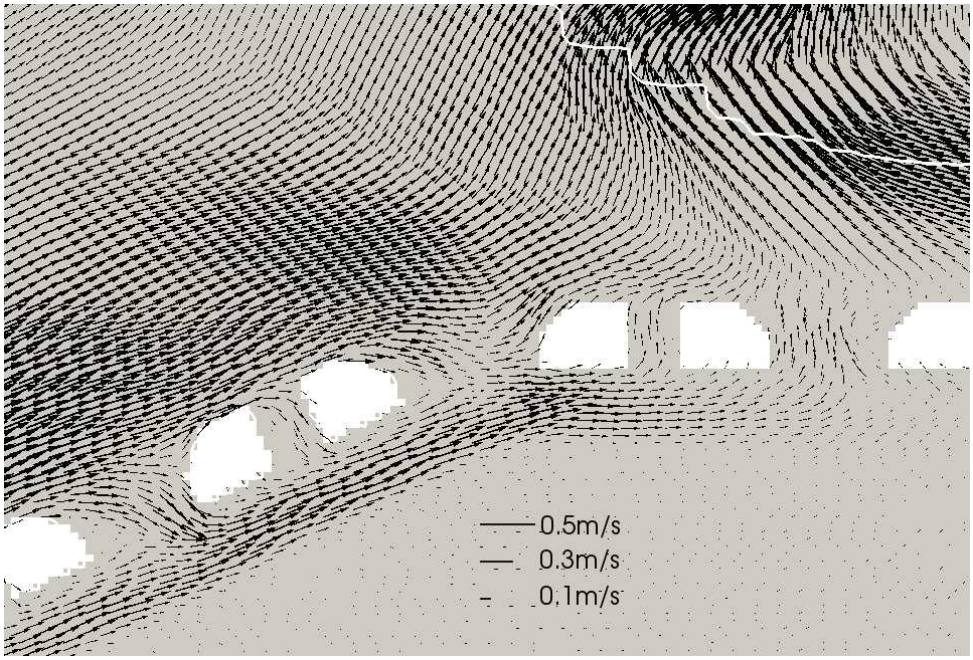

(b) t=8.1s

Figure 8. Snapshot of the flow around the shoulder of the slope.

Numerical Computation of 2-D Flow Field

A numerical wave flume CADMAS-SURF was used for reproducing the 2-D flow field around the breakwater. Figure 9 shows a computational domain that is 23m long and 0.8m high. A submerged breakwater was installed at 10m from the wave source. Wave damping areas were added to prevent reflected waves stemming from both ends of the flume. Horizontal and vertical grid spacing Δx and Δz in the offshore region were set to 2.0cm and 1.0cm respectively, while near the breakwater, Δx was set to 1.0cm. The water depth h was 25cm. The submerged depth R was set to 2, 3, 4, 7, 10cm. The significant wave period $T_{1/3}$ was 2.0s. The total duration used for the analysis was 204.8s. The time step was automatically set to satisfy CFL condition. Boundary conditions for the velocity and pressure were SLIP while for the VOF function F, it was FREE.

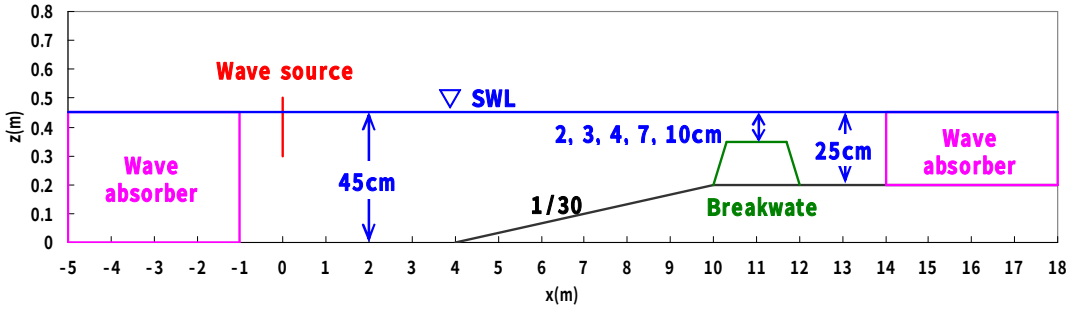

Figure 9. Computation domain.

Wave Force and Stabilizing Force

Wave force acting on an armor block was calculated by the following Morison formula:

$$F = F_D + F_I = \frac{1}{2} C_D \rho_W S_t u_t |u_t| + C_M \rho_W V \frac{du_t}{dt} \tag{4}$$

where F_D is the drag force, F_I is the inertia force. The magnitude of drag and inertia force can be evaluated as follows (for example Hiramatsu and Sato, 2010). If we use long wave approximation, the maximum drag force F_{Dmax} and the maximum inertia force F_{Imax} acting on the single cube can be expressed as follows:

$$F_{D\max} = \frac{1}{8} C_D \rho_w V^{2/3} g \frac{H^2}{h} \tag{5}$$

$$F_{I\max} = C_M \rho_w V \frac{H\pi}{T} \sqrt{\frac{g}{h}} \tag{6}$$

Suppose the structure is constructed within the breaker zone and the magnitude of the drag and inertia coefficient is comparable, one obtains

$$\frac{F_{D\max}}{F_{I\max}} = \frac{0.78}{8\pi} \frac{C_D}{C_M} \frac{\sqrt{ghT}}{V^{1/3}} = \frac{L}{32 D_n} \tag{7}$$

where h is the water depth, T is the wave period, H is the wave height, L is the wave length. From the equation above, it can be recognized that the inertia force is predominant when L/D_n is smaller than 32. For example, the typical experimental condition adopted in the hydraulic model experiment described above, *e.g.*, the submerged depth R=5cm, the significant wave period $T_{1/3}$=2.0s and the length of the armor block D_n=0.045m gives the ratio $L_{1/3}/D_n$=31. Therefore it is significant to include the inertia force as well as the drag force in the prediction model.

Figure 10 schematically shows the definition of the stabilizing force expressed by the following equation.

$$F_S(t) = \begin{cases} C_E \mu \left(W - F_n(t) \right) & \text{(crown)} \\ C_R C_E \left\{ W \sin\theta + \mu \left(W \cos\theta - F_n(t) \right) \right\} & \text{(slope)} \end{cases} \tag{8}$$

where θ is the slope angle, μ is the friction factor with the value of 0.6, W is the weight of the block in water. C_E represents the shading effect with the value larger than 1.0. C_R represents the structural weakness of the armor block at the top of the slope. The value of C_R is 1.0 for the lower and middle position of the slope while it is smaller than 1.0 for the top of the slope. The value of C_E was determined to be 3.5 thorough sensitivity analyses. The value of C_R was decided to be 0.3 for the two blocks at the top of the slope. Combination of these values gave good agreement between the experimental results and simulated ones.

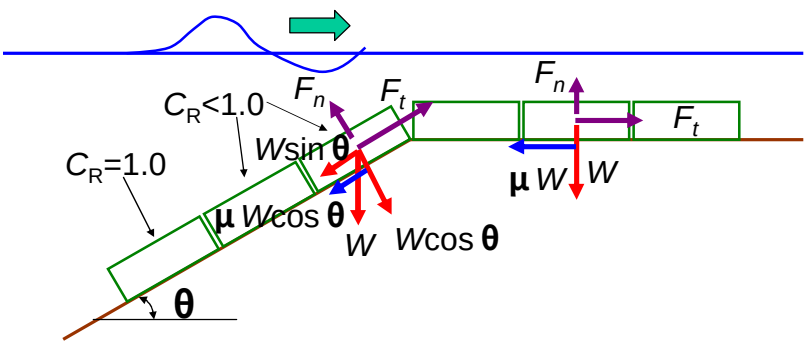

Figure 10. Definition of the stabilizing force.

COMPARISON BETWEEN PREDICTION AND EXPERIMENT

Possible Existence Range of the Critical Stability Number

Figure 11 shows an example of the spatial distributions of the ratio of one-tenth highest wave force to stabilizing force where the water depth was 10cm. If the ratio exceeds 1.0, the block of corresponding location will move. The critical condition exists between H_s=13.9cm and 14.6cm. The ratio shows its maximum value at the top of the slope. It shows a large value at the crown of the breakwater again, and then it decreases rapidly at the onshore position of the crown. According to the design manual for coastal facilities (2000), the mass of armor material in the onshore position of the crown can be reduced. The calculated distribution shown in Figure 11 agrees qualitatively with the description in the design manual.

Figure 12 shows the possible existence range of the critical stability number obtained by the experiment and the prediction model. When the submerged depth R is 4 to 10cm, namely $R/H_{1/3}$ is larger than 0.3, the critical stability numbers obtained by the proposed model agree well with the experimental results. However, when the submerged depth is smaller than 3cm, namely, $R/H_{1/3}$ is around 0.2, the proposed model underestimates the stability.

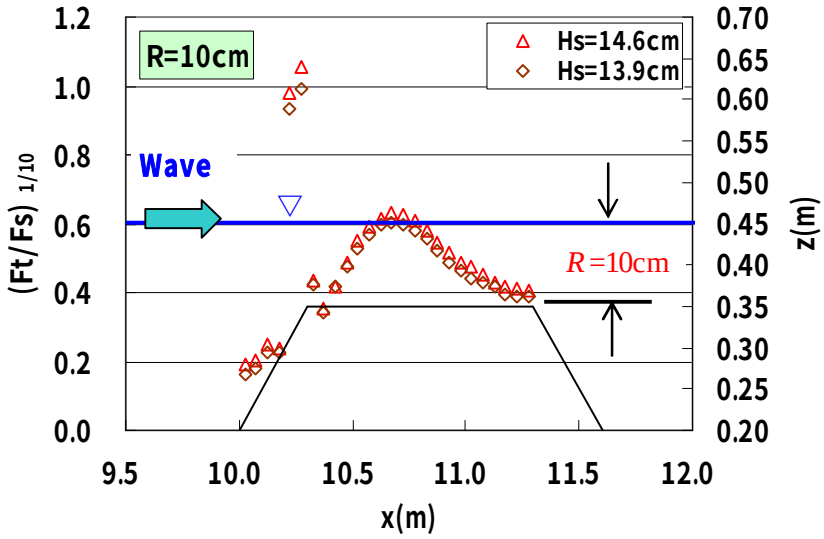

Figure 11. Spatial distributions of the ratio of wave force to stabilizing force (*R*=10cm).

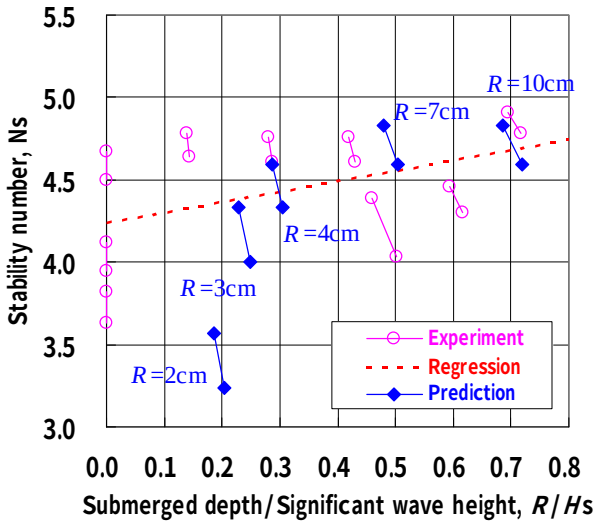

Figure 12. Possible existence range of the critical stability number.

Effect of the Duration of Wave Force on the Predicted Stability

Figure 13 shows the time series of the water level, the tangential flow velocity around the shoulder of the slope and the tangential wave force acting to the block placed at the top of the slope where the submerged water depth R was 2cm and the significant wave height H_S was 10.8cm. The broken line in the upper figure indicates the elevation of the crest level of the breakwater. In the present case, the ratio of one-tenth highest wave force to stabilizing force exceeded 1.0. Therefore the block of corresponding location was judged to move. An impulsive wave force with short duration occurred just after the breakwater appeared in the air. This is one possible reason why the proposed model underestimates the block stability. In such a situation, even if the peak value was large, the impulse was not so large.

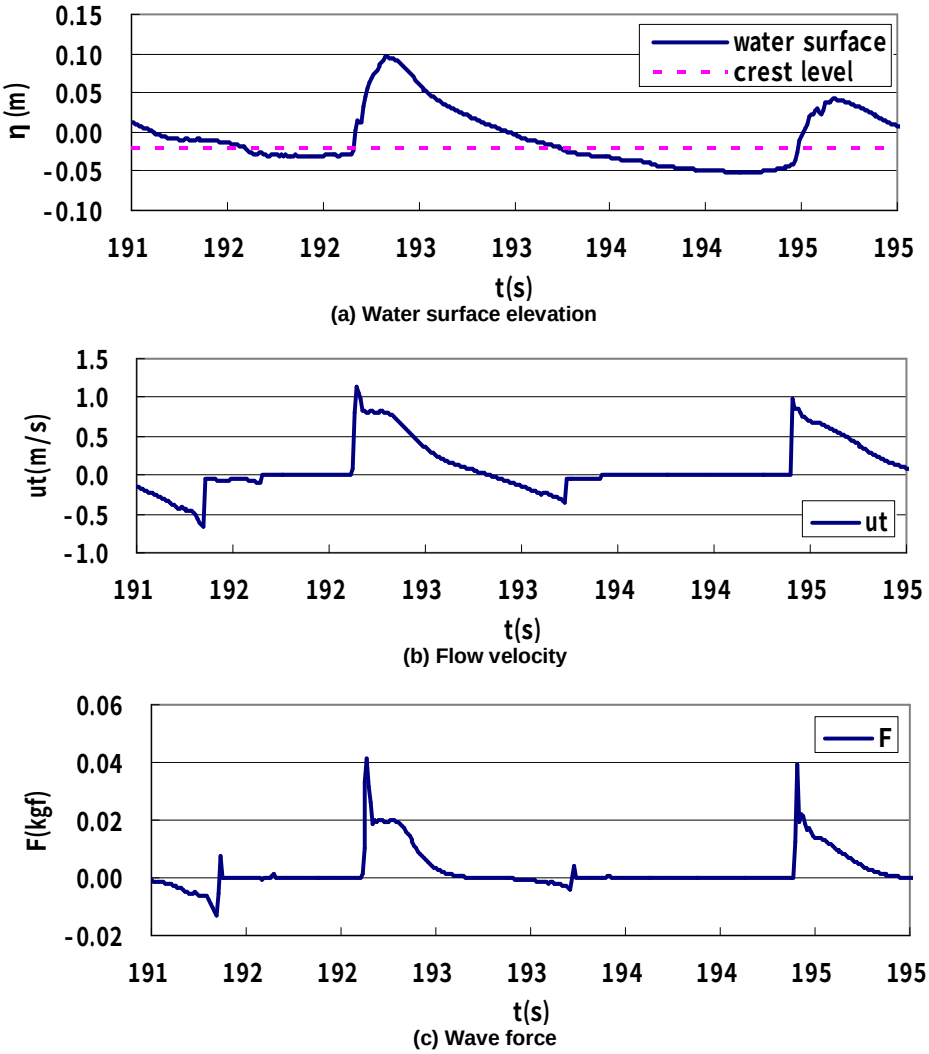

Figure 13. Time series of water surface elevation, flow velocity and the wave force. (R=2cm, H_s=10.8cm, Top of the slope)

To estimate the displacement of the block, the equation of the motion of the block was solved. The equation of the motion is expressed by the following form:

$$m\frac{d^2x}{dt^2} = F_t(t) - C_R C_E F_{S0}(t) = F_t(t) - C_R C_E \{W\sin\theta + \mu(W\cos\theta - F_n(t))\} \tag{9}$$

where m is the mass of the block, x is the displacement of the block, t is the time, $F_t(t)$ is the tangential wave force. The time series of the block position was obtained by the integration of this equation. In the present analysis, variation of the fluid force due to the change of the block position was not taken into account.

Figures 14 and 15 show the calculated results of the displacement of the armor block in the shallow submerged water case with R = 2cm and the deep submerged water case with R = 10cm respectively. In these figures, the time series in the total tangential force acting on the armor block, the acceleration of the block and the displacement of the block are indicated. The peak values of the tangential wave forces of these two cases are almost identical with the value of 0.08N. However the duration of the action is different. The wave force of the shallow water case acted as an impulsive force with short duration while that for the deep water case acted rather a long duration. As a result, the displacement in the shallow water case is only 2mm. It is thought that the movement of the block is not detected in the model experiment when the sliding distance is smaller than the joint spacing of the block. On the other hand, the sliding distance of deep water case reached to 52mm. This value was large enough to be detected as damage in the model experiment.

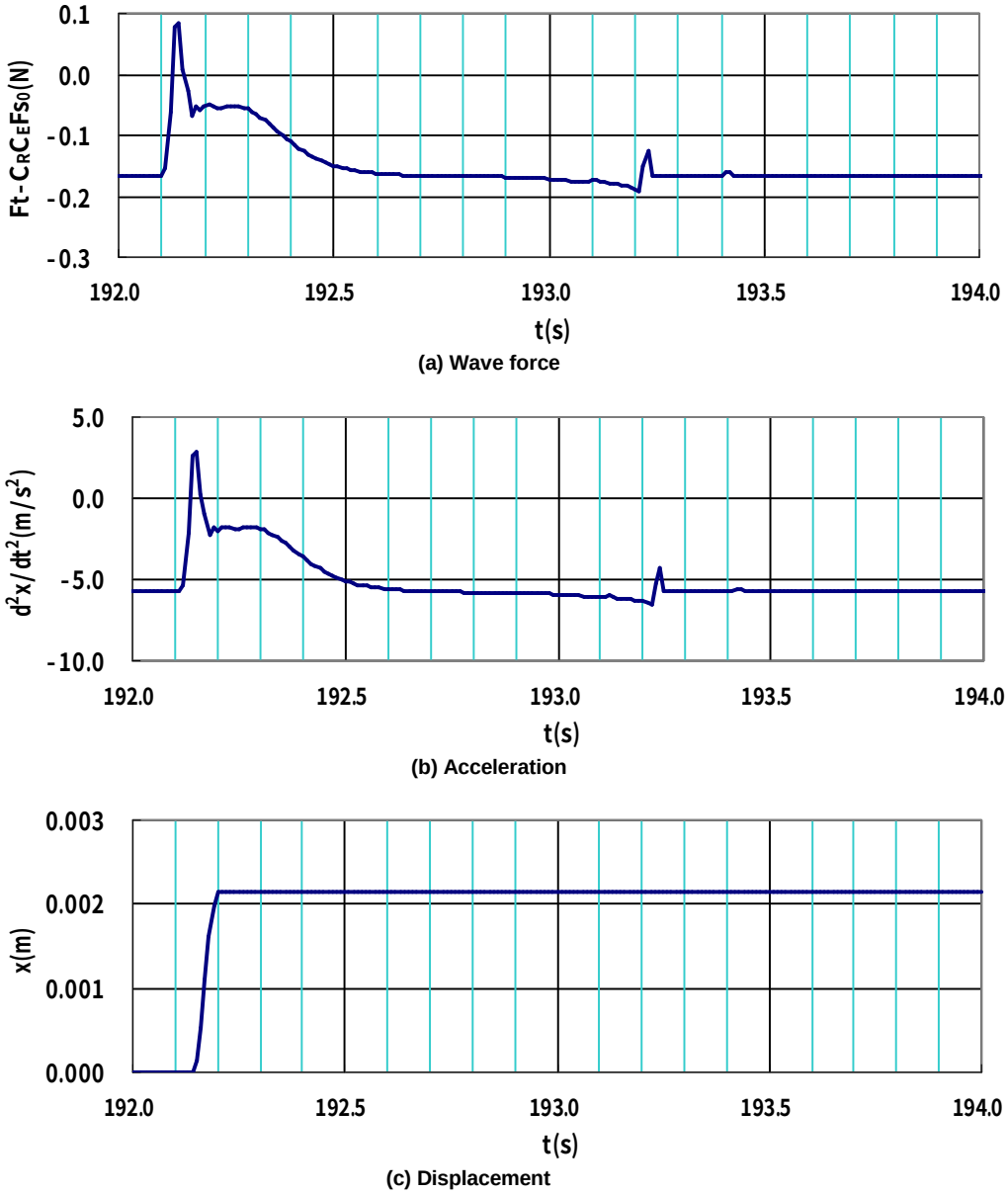

Figure 14. Time series of wave force, acceleration and displacement of the armor block. (R=2cm, H_s=10.8cm, Top of the slope)

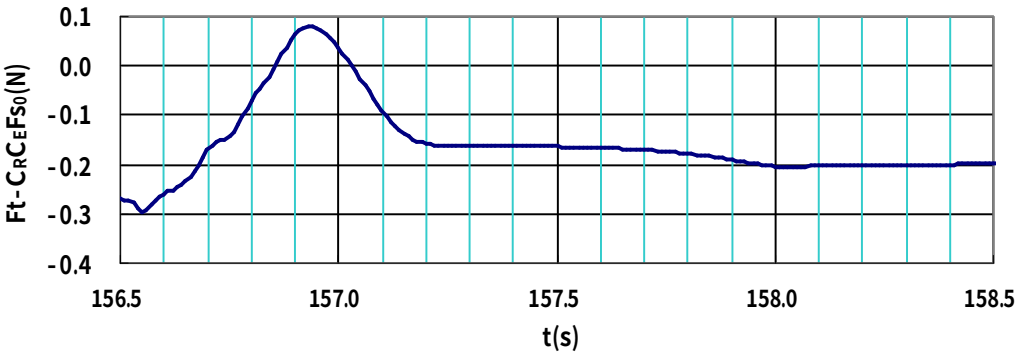

(a) Wave force

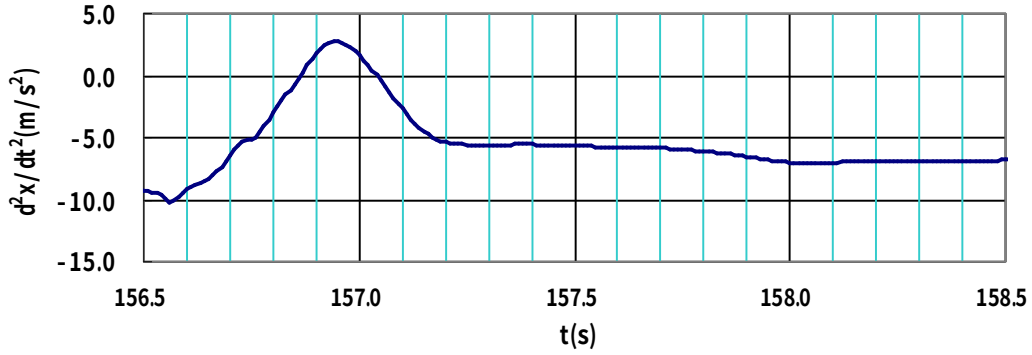

(b) Acceleration

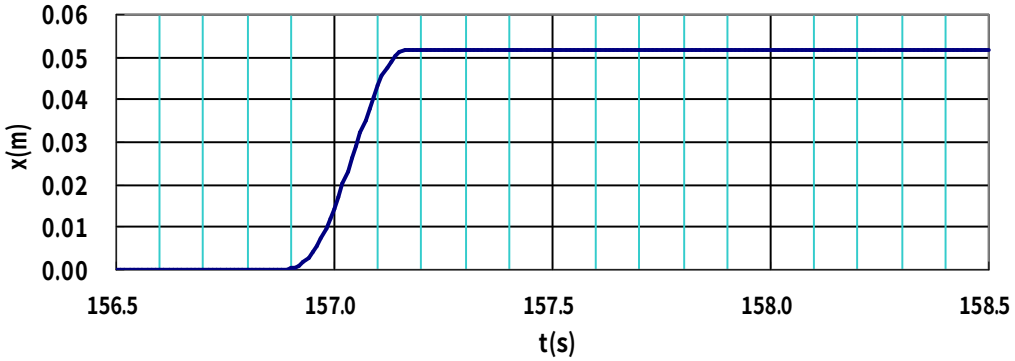

(c) Displacement

Figure 15. Time series of wave force, acceleration and displacement of the armor block. (*R*=10cm, H_s=14.6cm, Top of the slope)

Figures 16 shows the calculated time histories of the amount of the sliding distance. The significant wave heights used for the calculation were minimum wave height with damage, i.e., the wave heights correspond to the predicted upper stability number connected by the solid line as shown in Figure 12. Intermittent sliding of armor block is observed. The frequency of the occurrences of sliding increased and the sliding length decreased as the submerged depth decreased. From these results, it can be concluded that the proposed prediction method tends to underestimate the armor block stability when the wave force is impulsive with short duration.

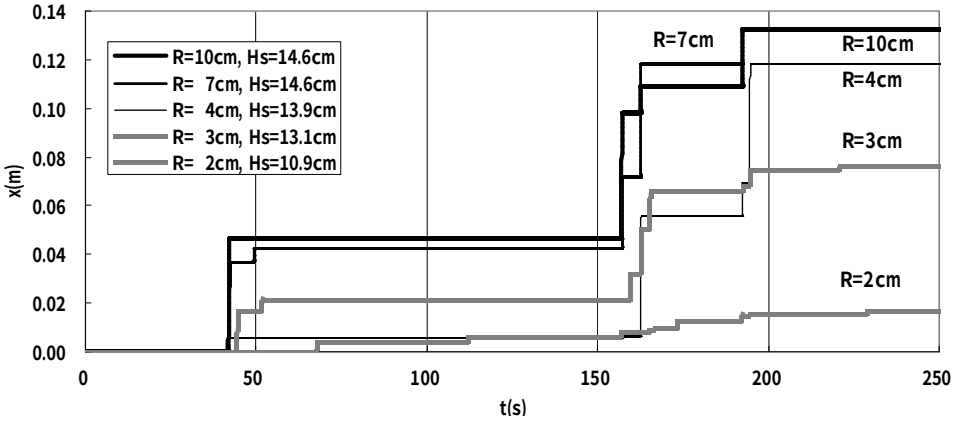

Figure 16. Time histories of sliding distances.

CONCLUDING REMARKS

To sum up the main results of this study, the following conclusions can be made:

1) An evaluation method for the critical condition on armor block stability for submerged breakwaters is proposed. Parameters for the evaluation were calibrated through comparison between experimental and numerical results.

2) The spatial distribution of the ratio of wave force to the stabilizing force agrees qualitatively with the distribution of the required mass of armor units on the crown of the breakwater. That is to say, the proposed method can determine the required mass of armor block space to space.

3) When R/Hs was larger than 0.3, the proposed method well reproduced the experimental results, while it underestimated the stability when R/Hs was around 0.2.

4) An impulsive wave force with short duration acted when the water depth above the breakwater was shallow. In such a situation, even if the peak value was large, the impulse was not so large. To estimate the displacement of the block, the equation of the motion of the block was solved.

REFERENCES

Asakawa, T., Sato, H., Kuchinomachi, M. and M. Noguchi, 1992. Experimental study on stability of concrete armour units for artificial reefs. *Proceedings of Coastal Engineering*, JSCE, Vol.39, pp.656-660, (in Japanese).

CIRIA (Construction Industry Research and Information Association), 1991. *Manual on the use of rock in coastal and shoreline engineering*. CIRIA Special publication 83, A.A.ALKEMA Publishers, 607p.

Hiramatsu, H. and S. Sato, 2010. Stability and Beach Erosion Control Performance of Submerged Sand Pack Breakwater. *Journal of JSCE*, Ser. B2 (Coastal Engineering), Vol.66, pp.656-660. (in Japanese).

Hudson, R. Y., 1959. Laboratory investigation of rubble-mound breakwaters. *Proc. ASCE*, Vol.85, WW3, pp.93-121.

Isobe, M., Takahashi, S., Yu, S. P., Sakakiyama, T., Fujima, K., Kawasaki, K., Jiang, Q., Akiyama, M. and H. Oyama, 1999. Interim report on development of numerical wave flume for maritime structure design. *Proceedings of Civil Engrg in the Ocean*, Vol.15, pp. 321-326, JSCE., (in Japanese).

Japan Society of Civil Engineers, 2000. *Design Manual for Coastal Facilities*, Maruzen Co., Ltd., 577p.

Kondo, M., Arikawa, T., Seki, K. and H. Murakawa, 2009. Damage Mechanism of Armor Units at the Breakwater Head Using the 3D Numerical Wave Tank. *Journal of JSCE*, Ser. B2 (Coastal Engineering), Vol.65, pp.861-865. (in Japanese).

Matsumoto, A., Yamamoto, M. and A. Mano, 2011a. Evaluation of the Critical Condition on Armor Block Stability for Submerged Breakwaters, *Proceedings of Coastal Structures* 2011, ASCE. Yokohama, in press.

Matsumoto, A., Yamamoto, M. and A. Mano. 2011b. A Light Concrete Block Stabilized by Distributed Holes for Submerged Breakwaters. *Journal of Coastal Research*, Special Issue 64, pp.567-571.

Nakayama, A., 1993. Experimental study on hydraulic characteristics and stability of artificial reef, *Proceedings of Coastal Engineering*. JSCE, Vol.40, pp.816-820, (in Japanese).

Noguchi, K., Torii, K., Hitomi, H., Fueta, S., Maruyama, J., Kisida, H. and S. Yamasaki, 2002. Nationwide investigations on artificial reef and gentle slope-type coastal dike. *Proceedings of Coastal Engineering*, JSCE, Vol.49, pp. 921-925. (in Japanese).

Okamoto, S. and S. Kawano, 1993. Experimental study on the damage mechanism of armor units of artificial reefs. *Proceedings of Coastal Engineering*, JSCE, Vol.49, pp. 921-925. (in Japanese).

Okuma, Y., Kyono, T., Shibasaki, N., Yasuda, K. and O. Nakano, 2003. Study on Cover Block Stability of Caisson Considered Difference of Damaged Degree Based on Wave Velocity. *Proceedings of Coastal Engineering*, JSCE, Vol.50, pp.751-755, (in Japanese).

Open CFD Ltd., 2011. URL: http://www.openfoam.com/; accessed on December 13, 2011.

Van der Meer, J. W., Allsop, N. W. H., Pilarczyk, K. W., Stam, C. -J., Powell, K. and Burcharth, H., 1991. *Manual on the use of rock in coastal and shoreline engineering*, CIRIA, Special Publication 83, CUR Report l54, pp. 269-270.

Van der Meer, J.W. and K.W. Pilarczyk, 1990. Stability of low-crested and reef breakwaters. *Proceedings of the 22th International Conference on Coastal Engineering* (Delft, the Netherlands), pp. 1375-1388.

Vidal, C., Losada, M.A. and E.P.D. Mansard, 1995. Stability of low-crested rubble-mound breakwater heads. *Journal of Waterways, Port, Coastal, and Ocean Engineering*, Vol.121, No.2, pp. 114-122.

Vidal, C., Medina, R. and F.L. Martin, 2000. A methodology to assess the armor unit stability of low-crested and submerged rubble-mound breakwaters. *Proceedings of the Coastal Structures* '99 (Santander, Spain), pp. 721-725.

Yamamoto M. and Asakawa T., 1982. Stability analysis for rubble-mound foundation through irregular wave test, *Proceedings of the 18th International Conference on Coastal Engineering* (Cape Town, South Africa), pp. 2129-2143.